International Journal of Digital Earth

ISSN: 1753-8947 (Print) 1753-8955 (Online) Journal homepage: https://www.tandfonline.com/loi/tjde20

Evapotranspiration partitioning using an optimality-based ecohydrological model in a semiarid shrubland

Lajiao Chen, Liying Sun, Weijiang Liu, Lizhe Wang, Hui Wu, A-Xing Zhu & Yiqi Luo

INTERNATIONAL JOURNAL OF DIGITAL EARTH
https://doi.org/10.1080/17538947.2018.1503741

Evapotranspiration partitioning using an optimality-based ecohydrological model in a semiarid shrubland

Lajiao Chen[a], Liying Sun[b], Weijiang Liu[c], Lizhe Wang[a,d], Hui Wu[e,f], A-Xing Zhu[g,h] and Yiqi Luo[i]

[a]Institute of Remote Sensing and Digital Earth, Chinese Academy of Sciences, Beijing, People's Republic of China; [b]Institute of Geographic Sciences and Natural Resources Research, Chinese Academy of Sciences, Beijing, People's Republic of China; [c]Chinese Academy For Environmental Planning, Beijing, People's Republic of China; [d]Computer Science and Geological Survey of CUG, China University of Geosciences, Wuhan, People's Republic of China; [e]Smart City Research Center, Hangzhou Dianzi University, Hangzhou, People's Republic of China; [f]Smart City Research Center of Zhejiang Province, Hangzhou, People's Republic of China; [g]Jiangsu Center for Collaborative Innovation in Geographical Information Resource Development and Application, School of Geography, Nanjing Normal University, Nanjing, People's Republic of China; [h]Department of Geography, University of Wisconsin–Madison, Madison, WI, USA; [i]Center for Ecosystem Science and Society, Northern Arizona University, Flagstaff, AZ, USA

ABSTRACT

Partitioning of evapotranspiration (ET) into biological component transpiration (T) and non-biological component evaporation (E) is crucial in understanding the impact of environmental change on ecosystems and water resources. However, direct measurement of transpiration is still challenging. In this paper, an optimality-based ecohydrological model named Vegetation Optimality Model (VOM) is applied for ET partitioning. The results show that VOM model can reasonably simulate ET and ET components in a semiarid shrubland. Overall, the ratio of transpiration to evapotranspiration is 49% for the whole period. Evaporation and plant transpiration mainly occur in monsoon following the precipitation events. Evaporation responds immediately to precipitation events, while transpiration shows a lagged response of several days to those events. Different years demonstrate different patterns of T/ET ratio dynamic in monsoon. Some of the years show a low T/ET ratio at the beginning of monsoon and slowly increased T/ET ratio. Other years show a high level of T/ET ratio for the whole monsoon. We find out that spring precipitation, especially the size of the precipitation, has a significant influence on the T/ET ratio in monsoon.

ARTICLE HISTORY
Received 25 April 2018
Accepted 18 July 2018

KEYWORDS
ET partitioning; optimality-based ecohydrological model; VOM; semiarid shrubland

1. Introduction

Evapotranspiration (ET) refers to water transferred from land surface to the atmosphere, which is closely associated with land surface-atmosphere exchanges of water, carbon and energy (Oki and Kanae 2006; Trenberth, Fasullo, and Kiehl 2009; Wang and Dickinson 2012). ET is composed of transpiration (T) from vegetation (biological component) and evaporation (E) from land surfaces (non-biological component). ET partitioning is crucial to examine how water and carbon cycles are coupled, which is essential in understanding the impact of climate change and human activities on ecosystems and water resources (Newman et al. 2006; Lawrence et al. 2007; Cao et al. 2010; Scott and Biederman 2017). Plants lose water when they exchange for carbon through stoma

CONTACT Lizhe Wang wanglz@radi.ac.cn Institute of Remote Sensing and Digital Earth, Chinese Academy of Sciences, Beijing 100094, People's Republic of China; Computer Science and Geological Survey of CUG, China University of Geosciences, Wuhan 430074, People's Republic of China

during photosynthesis, hence T is intrinsically coupled with plant productivity. The impact of climate change including the variation of temperature and precipitation on vegetation alters transpiration and hence plant productivity (Dirmeyer et al. 2006; Lawrence et al. 2007). Therefore, accurate estimation of ET components is highly needed to evaluate how vegetation responds to climate change, particularly in water-limited ecosystems (Ponce-Campos et al. 2013; Biederman et al. 2017).

It is challenging to estimate E and T separately due to the lacking of data (Scott et al. 2006). In recent years, several approaches are developed for ET partitioning, including measuring and modeling methods (Scott et al. 2006; Cavanaugh, Kurc, and Scott 2011; Raz-Yaseef et al. 2012; Kool et al. 2014). For measuring approaches, sap flow and chambers are widely applied for T measurement while micro-lysimeters and soil chambers are used for E estimation (Evett, Warrick, and Matthias 1995; Todd et al. 2000; Domec et al. 2012). Moreover, isotope measurements have been introduced for ET partitioning and have demonstrated great potential (Wang et al. 2010). However, those direct measurements are costly, laborious and with low time resolution, which highly limited their applications. With the recent development of measurement techniques, eddy covariance (EC) has demonstrated its potential for ET partitioning (Zhou et al. 2016; Zhou et al. 2018). Zhou et al. (2016) suggested ET partitioning can be achieved based on the concept of underlying water use efficiency using eddy covariance measurements. Such method could be used easily for ET partitioning for different time scales and vegetation types with the EC measurements.

Apart from direct measurements, modeling is a promising approach for ET partitioning. Models that calculate evaporation and transpiration respectively can be used for ET partitioning, such as Shuttleworth-Wallace (S-W) model (Shuttleworth and Wallace 1985), ENWATAL (Evett and Lascano 1993), and Cupid-DPEVAP (Thompson et al. 1997). Note that most of the existing models treat ET as if it is a physical process controlled by energy, vapor pressure, and turbulence (Schymanski et al. 2007; Sivapalan 2009). The way to treat ET as a physical process rather than as a biological process is unrealistic and questionable. The inability to simulate detailed process feedbacks of eco-hydrological processes in these models restricts the models' capacity to capture coupled dynamics of watersheds and ecosystems. In addition, these models usually have a high requirement on the spatial and temporal parameterization of vegetation physiological variables. In recent years, models based on optimality principles have merged, providing a promising alternative for ET estimation. These kinds of models are based on an optimality hypothesis that the natural selection of vegetation leads to the optimal use of resources such as water, light, and CO_2 (Eagleson 2002). Utilization of a specific optimality principle (such as maximization of primary productivity, or minimization of water stress) allows the development of an objective function to define optimality, along with constraints such as water, carbon, and energy balance (Rodriguez-Iturbe and Porporato 2004). The advantage of these kinds of models is that they can realistically describe the coupling relationship of transpiration and photosynthesis on a biological basis (Wang et al. 2007; Pauwels et al. 2007; Van der Tol et al. 2008; Caylor, Scanlon, and Rodriguez-Iturbe 2009; Schymanski et al. 2009). However, till now the optimality-based models are still at the very outset; hence, it is essential to examine the optimality principle in more conditions and more ecosystems (Kerkhoff, Martens, and Milne 2004).

This paper, therefore, applied an optimality-based ecohydrological model for ET partitioning in a semiarid ecosystem to better understand the response of evaporation and transpiration to climate characteristics. The study is conducted in a Chihuahuan Desert shrubland site in USDA-ARS Walnut Gulch Experimental Watershed (WGEW) in southeastern Arizona, USA, with nine years of detailed measurements, including meteorological data and water flux data. We use the measured ET data to validate the simulated ET of the model. We then analyze the characteristics of evaporation and transpiration and their response to precipitation on different time scales. The influence of precipitation characteristic on monsoon T/ET ratio is examined.

2. Materials and methods

2.1. Site description

This study is conducted at the Lucky Hills site of USDA-ARS WGEW in southeastern Arizona (31° 44′37″ N, 110°3′5″ W) (Figure 1). The elevation is about 1372 m with slopes ranged from 3% to 8%. The climate is characterized by cool winters, warm summers and a bimodal precipitation pattern with the majority falling during the summer monsoon season (Goodrich et al. 2008). Mean annual temperature is 17°C, and annual precipitation is about 356 mm.

This site is a typical Chihuahuan Desert shrubland. Vegetation mainly consists of perennial C3 shrubs and the dominant shrubs are whitethorn acacia (*Acacia constricta*), tarbush (*Flourensia Cernua*), creosotebush (*Larrea tridentate* (DC.) Cov.), desert zinnia (*Zinnia pumila*), with some mariola (*Parthenium incanum*) and little leaf sumac (*Rhus microphylla*). The height of the shrub is about 0.3–1 m and the canopy coverage is about 51% (Scott et al. 2006). The ground between the shrub canopies is almost bare and rocky soil with very small amounts of herbs and grasses. The soil is gravelly sandy loam with a high percentage of rock.

2.2. Data

Data used in this study are obtained from Southwest Watershed Research Center (SWRC) of USDA through the governmental official website (http://www.tucson.ars.ag.gov/dap/). These data are used as model inputs and model validation (Table 1).

Model inputs refer to meteorological data, including precipitation, relative humidity, solar radiation, and temperature. Precipitation data are collected from the rain gauge station near the Lucky Hills flux site. The other meteorological data are gained at the meteorological station known as LhMet (31°44′8″ N, 110°3′8″ W) (Keefer, Moran, and Paige 2008). All of the meteorological data are measured every 20 minutes, which are scaled up to 1 h to satisfy the input requirement

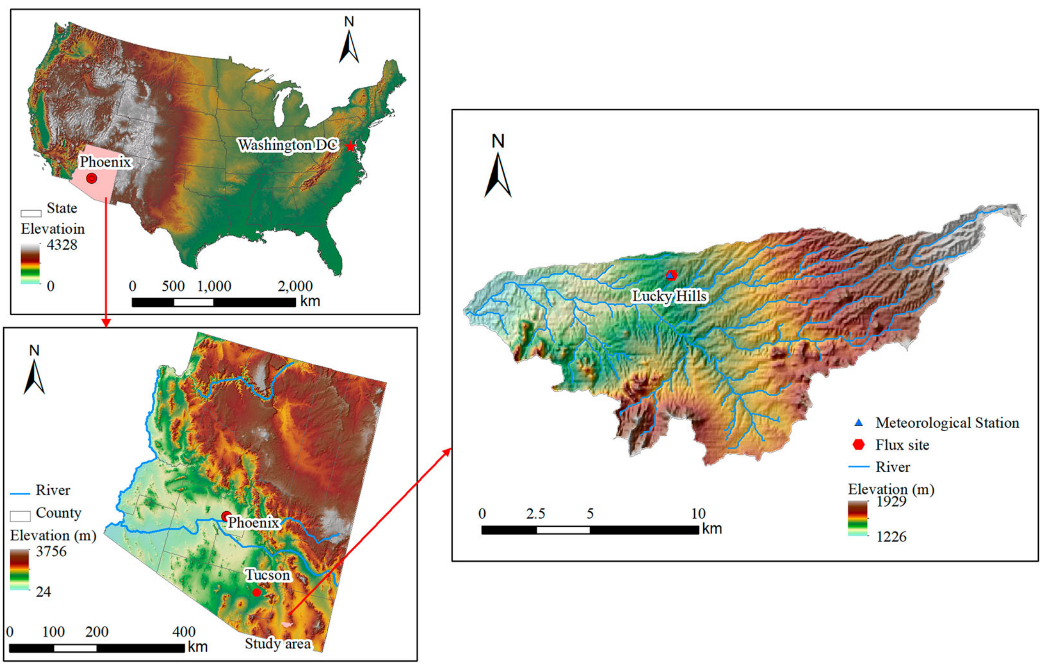

Figure 1. Location of the study area and measurement sites.

Table 1. Data used in this study.

Data type		Data items	Scale	Period
Inputs	Meteorological data	Solar radiation, temperature, precipitation, relative humidity, PAR	20 min, scaled up to 1 h	1998–2006
Validation	Flux data	Water vapor flux		
	Satellite data	NDVI	16-days	2000–2006

of ecohydrological model. Meteorological data are available from 1998 to 2006. The validation data include water vapor flux, CO_2 flux, and satellite data. The water vapor flux is acquired from the Bowen Ratio Energy Balance System (BREB, Model 023/CO_2, Campbell Scientific Inc., Logan, UT) (Emmerich and Verdugo 2008). In the BREB system, atmospheric gradients of air temperature, moisture, and CO_2 are measured every 10 s and averaged to 20 min. In order to be comparable with the model output, the measurements are scaled up to 1 day for model validation. The satellite data mainly refer to 16 days and 250 m resolution vegetation indices (MOD13Q1) from 2000 to 2006, which are downloaded from EROS Data Center, US Geological Survey (http://www.edc.usgs.gov/).

Both model inputs and validation data are quality controlled. For each data items, the outliers of the data are removed. For model inputs, the missing flux data need to be filled to force the long-term simulation. The missing flux data with small gaps less than 2 hours are filled using linear interpolation while the large gaps are filled with the Mean Diurnal Variation (MDV) method (Falge et al. 2001). The missing meteorological data are gap-filled by the nearby meteorological station.

2.3. Model description

The Vegetation Optimality Model (VOM) developed by Schymanski et al. (2009) is used in this study. VOM coupled a multilayered physically based water balance model and an ecophysiological gas exchange model (Figure 2). We list the most important equations as follows. For details of the model, please see the reference of Schymanski et al. (2009).

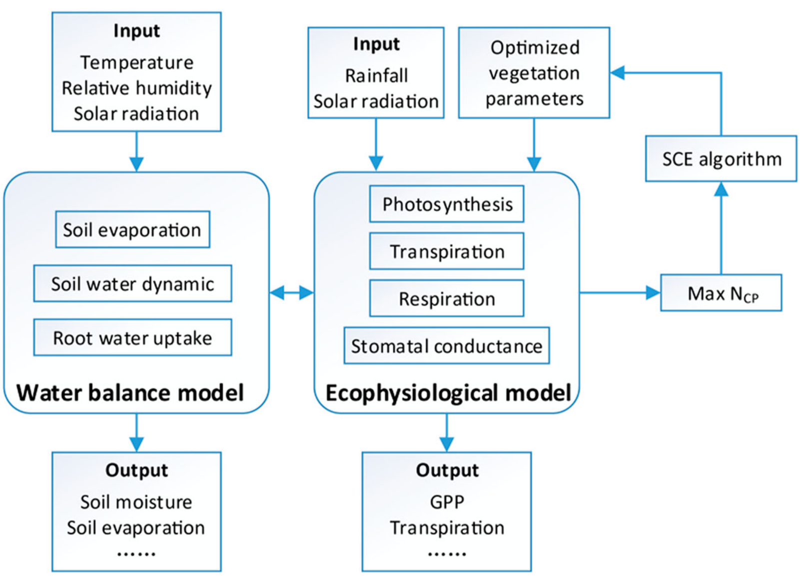

Figure 2. Structure of the VOM model.

2.3.1. Carbon assimilation: photosynthesis

CO_2 assimilation (A_g) is calculated following a physical canopy gas exchange model (Schymanski et al. 2007), which modifies the canopy as two big leaves representing the perennial and seasonal vegetation.

$$A_g = \frac{1}{8}(4C_aG_s + 8\Gamma_*G_s + J_A - 4R_l) - \frac{1}{8}\sqrt{(-4C_aG_s + 8\Gamma_*G_s + J_A - 4R_l)^2 + 16G_s\Gamma_*(8C_aG_s + J_A + 8R_l)} \tag{1}$$

where C_a is the mole fraction of CO_2 in the air, G_s is the stomatal conductivity, Γ_* is the CO_2 compensation point in the absence of mitochondrial respiration, and J_A is the photosynthetic electron transport rate.

2.3.2. Transpiration

Canopy transpiration is modeled as a diffusive process controlled by stomatal conductivity and governed by photosynthesis:

$$E_t = aG_s(W_l - W_a) = aG_sD_v \tag{2}$$

where D_v is the atmospheric vapor deficit, W_l and W_a denote the mole fraction of water vapor in air inside the leaf and in the atmosphere, which is approximate to D_v, and a is the molecular diffusion coefficient of CO_2 in the air, defined as 1.6.

Stomatal conductivity is estimated following the optimal hypothesis proposed by Cowan and Farquhar (1977). The hypothesis assumes that for any given amount of water in a period, a leaf can achieve maximum CO_2 uptake by adjusting G_s in a way that the slope of transpiration (E_t) and carbon assimilation (A_g) are maximized with a constant value of λ over the period.

$$\frac{\partial E_t/\partial G_s}{\partial A_g/\partial G_s} = \frac{\partial E_t}{\partial A_g} = \lambda \tag{3}$$

Combining Equations (1)–(3), vegetation transpiration can be calculated as

$$E_t = \frac{aD_v[C_a(J_A - 4R_l) - 4(J_A + 2R_l)\Gamma_*]}{4(C_a - 2\Gamma_*)^2} + \frac{\sqrt{3}\sqrt{aD_vJ_A\Gamma_*(\lambda C_a - 2aD_v + 2\lambda\Gamma_*)^2(\lambda C_a - aD_v + 2\lambda\Gamma_*)[C_a(J_A - 4R_l) - (J_A + 8R_l)\Gamma_*]}}{4(C_a + 2\Gamma_*)^2(\lambda C_a - aD_v + 2\lambda\Gamma_*)} \tag{4}$$

where λ including λ_s and λ_p is a constant within one day, and is parameterized as a function of the average matric suction head of each soil layer (h_i) in the root zone.

2.3.3. Soil evaporation

Soil evaporation includes two parts: evaporation from unsaturated area E_{su} and evaporation from saturated area E_{ss}:

$$E_{su} = \frac{I_g(1 - 0.8M_A)\omega_uS_{u,1}}{\lambda_E\rho} \tag{5}$$

$$E_{ss} = \frac{I_g(1 - 0.8M_A)\omega_o}{\lambda_E\rho} \tag{6}$$

where I_g is the global irradiance per unit horizontal area, ω_u is the unsaturated surface area fraction,

$S_{u,1}$ is the average saturation degree in the unsaturated area of the top soil layer, λ_E is the latent heat of vaporization at 20°C, set at 2.45×10^6 J kg^{-1}, and ρ is the density of water, set at 1000 kg/m^3.

2.3.4. Vegetation optimality principle

The optimality principle applied in the model is that vegetation maximizes 'Net Carbon Profit' (*NCP*) when adapting to the environment. *NCP* is defined as total CO_2 uptake of vegetation over the entire period, minus all identified maintenance costs of the organs assisting photosynthesis, including foliage, roots, and water transport tissues. The objective function for optimization is defined as follows:

$$NCP = \int_{t_{\mathrm{start}}}^{t_{\mathrm{end}}} (A_g(t) - R_f(t) - R_r(t) - R_v(t))\mathrm{d}t \tag{7}$$

Here, A_g is the CO_2 uptake by plants, R_f is the foliage cost of grasses and trees combined, R_r is the root cost of grasses and trees combined, and R_v is the cost associated with the vascular systems of grasses and trees combined.

2.3.5. Vegetation parameters optimality strategy

Adaption of vegetation to environment consists of long-term adaption, like perennial vegetation tends to obtain an optimal vegetated cover area when surviving to climatic trends, and short-term adaption, like vegetation adjust water use properties every day to gain more carbon profit every day. Therefore, the vegetation properties consist of long-term properties that are adapted to long-term environmental conditions and short-term properties that are adapted to respond to day-to-day changes of environmental conditions. The vegetation parameters that need to be optimized are listed in Table 2. Long-term vegetation properties include a fraction of area covered by perennial vegetation ($M_{A,p}$), the thickness of root zone of perennial vegetation ($y_{r,p}$), and water use parameters of perennial and seasonal vegetation ($c_{\lambda,p}$,$c_{\lambda e,p}$, $c_{\lambda f,s}$, $c_{\lambda e,s}$). Short-term vegetation properties include a fraction of area covered by seasonal vegetation ($M_{A,s}$), electron transport capacity of perennial and seasonal vegetation ($J_{\max 25,p}$, $J_{\max 25,s}$), and the root area depth distribution of perennial and seasonal vegetation ($S_{adr,i,p}$, $S_{adr,i,s}$). The Shuffled Complex Evolution (*SCE*) optimization algorithm developed by Duan, Gupta, and Sorooshian (1993, 1994) is used to achieve the optimal vegetation parameters that would maximize *NCP* over the entire period.

To optimize longer-term parameters, the model needs to run for the entire period numerous times to search for the parameters that can maximize *NCP*. The Shuffled Complex Evolution

Table 2. Vegetation parameters optimized in the model (Schymanski et al. 2009).

	Vegetation parameters	Time scale of variation
Long-term vegetation parameters	Fraction of area covered by perennial vegetation ($M_{A,p}$)	Constant over entire simulation period
	Thickness of root zone of perennial vegetation ($y_{r,p}$)	Constant over entire simulation period
	Water use parameters of perennial vegetation ($c_{\lambda f,p}$ $c_{\lambda e,p}$)	Constant over entire simulation period
	Water use parameters of seasonal vegetation ($c_{\lambda f,s}$ $c_{\lambda e,s}$)	Constant over entire simulation period
Short-term vegetation parameters	Fraction of area covered by seasonal vegetation ($M_{A,s}$)	Varying on a daily scale
	Electron transport capacity of perennial vegetation ($J_{\max 25,p}$)	Varying on a daily scale
	Electron transport capacity of seasonal vegetation ($J_{\max 25,s}$)	Varying on a daily scale
	Root area depth distribution of perennial vegetation ($S_{adr,i,p}$)	Varying on a daily scale
	Root area depth distribution of seasonal vegetation ($S_{adr,i,p}$,$S_{adr,i,s}$)	Varying on a daily scale

Table 3. Vegetation parameters for this study.

Parameters	Description	Value
$y_{r,s}$	Thickness of root zone of seasonal vegetation (m)	1
a	Initial slope of quantum yield of electron transport (mol/mol)	0.1
H_a	Rate of exponential increase of *Jmax* with temperature (J/mol)	159,500
H_d	Rate of exponential decrease of *Jmax* with temperature (J/mol)	200,000
T_{opt}	Optimum temperature for electron transport (K)	305
c_{rv}	Proportionality constant for water transport carbon costs (mol/m^3)	$2.2*10^{-6}$
tcf	Turnover cost factor for foliage (mol/m^2/s)	$2.2*10^{-7}$
c_{rl}	Leaf respiration coefficient	0.07
c_{Rr}	Root respiration rate per volume of fine roots	$1.7*10^{-3}$
rurfmin	Minimum root surface area (m^2/m^3)	0.08
rurfinit	Initial root surface area (m^2/m^3)	0.08
r_r	Mean radius of fine roots (m)	$0.3*10^{-3}$
growthmax	Parameter determining the maximum daily growth increment of root surface are	0.1
prootmg	Constant root balance pressure of 1.5 MPa in grasses	150

optimization algorithm developed by Duan, Gupta, and Sorooshian (1993, 1994) is used to achieve the optimal vegetation parameters.

Short-term vegetation parameters are supposed to change dynamically on a daily basis. The optimality of these parameters is carried out by computing daily NCP_d each day to search for a value that may increase NCP_d. The daily increment of $M_{A,s}$ is set to 0.02 while the daily increment of $J_{max25,p}$, $J_{max25,p}$ is set to 1%. The fine root surface area distributions of perennial and seasonal plants ($S_{adr,i,p}$, $S_{adr,i,s}$) are optimized separately on a daily scale to allow adequate root water uptake with the lowest possible total root surface area. The model calculates *NCP* for every day using different combinations of these parameters. Only the combination that led to the maximum NCP_d on the previous day is then set to the subsequent day.

2.4. Model parameterization

2.4.1. Physical setting and parameter specification

The VOM model is applied to Lucky Hills site for 9 years from 1998 to 2006 with a time step of 1 hour. Parameters required by VOM model mainly contain parameters that vary with vegetation type and soil type.

Vegetation parameters that need to be specified include the rate of exponential increase of *Jmax* with temperature, the rate of exponential decrease of *Jmax* with temperature, optimal temperature for electron transport, leaf respiration rate, etc. These parameters (in Table 3) are prescribed according to the average value of C3 shrub with previous studies (Rodriguez-Iturbe and Porporato 2004; Schymanski et al. 2007; Lei et al. 2009).

The soil parameters used in the model are shown in Table 4. These soil parameters are specified according to the reference of Scott et al. 2000. In the VOM model, the soil profile is subdivided into sublayers but the van Genuchten soil parameters of each layer are treated as one value. Therefore, we then average the soil parameters of each sub-layer from the work of Scott et al. (2000) and obtain one value for the whole soil profile.

Table 4. Soil parameters for this study.

Parameters	Description	Value
Z	Average depth of the pedosphere (m)	2.5
Δ	Thickness of soil sublayers (m)	0.5
K_{sat}	Saturated hydraulic conductivity (mm/s^{-1})	$1.28*10^{-5}$
a_{vG}	Soil parameter of Van Genuchten water retention	7.5
n_{vG}	Soil parameter of Van Genuchten water retention	1.89
θ_r	Residual soil water content (m^{-3}/m^{-3})	0.065
θ_s	Statured soil water content (m^{-3}/m^{-3})	0.36

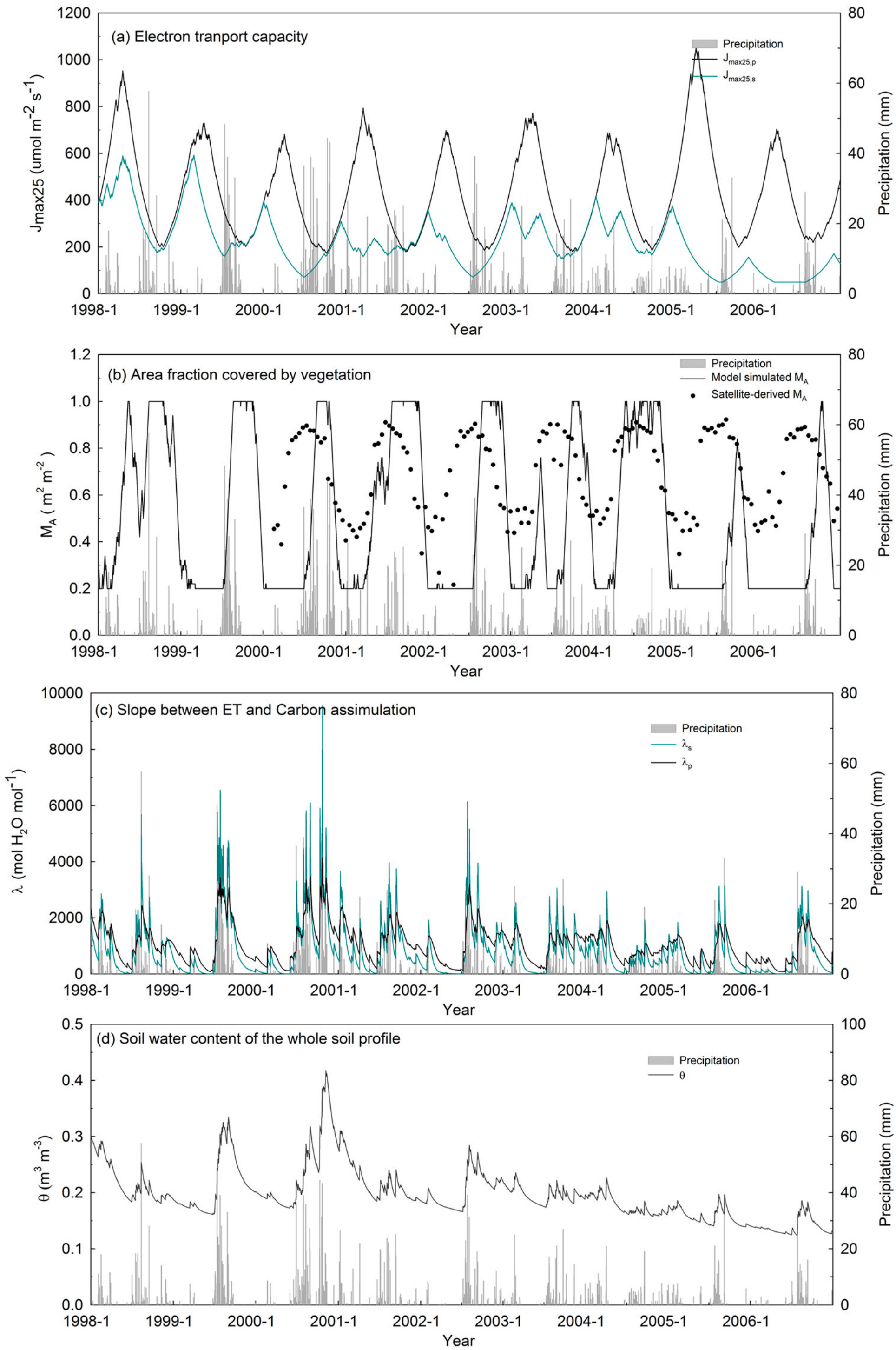

Figure 3. Simulated seasonal dynamic of vegetation properties with observed rainfall.

2.4.2. Optimized vegetation properties

With the specified parameters, the model is first applied to achieve the optimal vegetation parameters using *SCE* optimization algorithm. The *NCP* is about 130.2 mol/m^2 for the 9 years. The optimized vegetation properties are shown in Figure 3. The daily optimized J_{max25} of seasonal and perennial vegetation are shown in Figure 3(a), which seems to follow a similar seasonal dynamics pattern with precipitation (Figure 3(d)). The J_{max25} increased when a precipitation event occurs and soil water increases, and the J_{max25} drops as the soil water drops.

Simulated foliage vegetation cover fraction M_A (Figure 3(b)) ranged from 0.2 to 1.0. It is validated by satellite-derived M_A, which is obtained using the following equation:

$$M_A = (NDVI - NDVI_s)/(NDVI_v - NDVI_s) \tag{8}$$

Here, $NDVI_s$ is the *NDVI* value of the pixels totally covered by soil, $NDVI_v$ is the *NDVI* value of pixels totally covered by vegetation. In this study, $NDVI_s$ is 0 while $NDVI_v$ is 0.92.

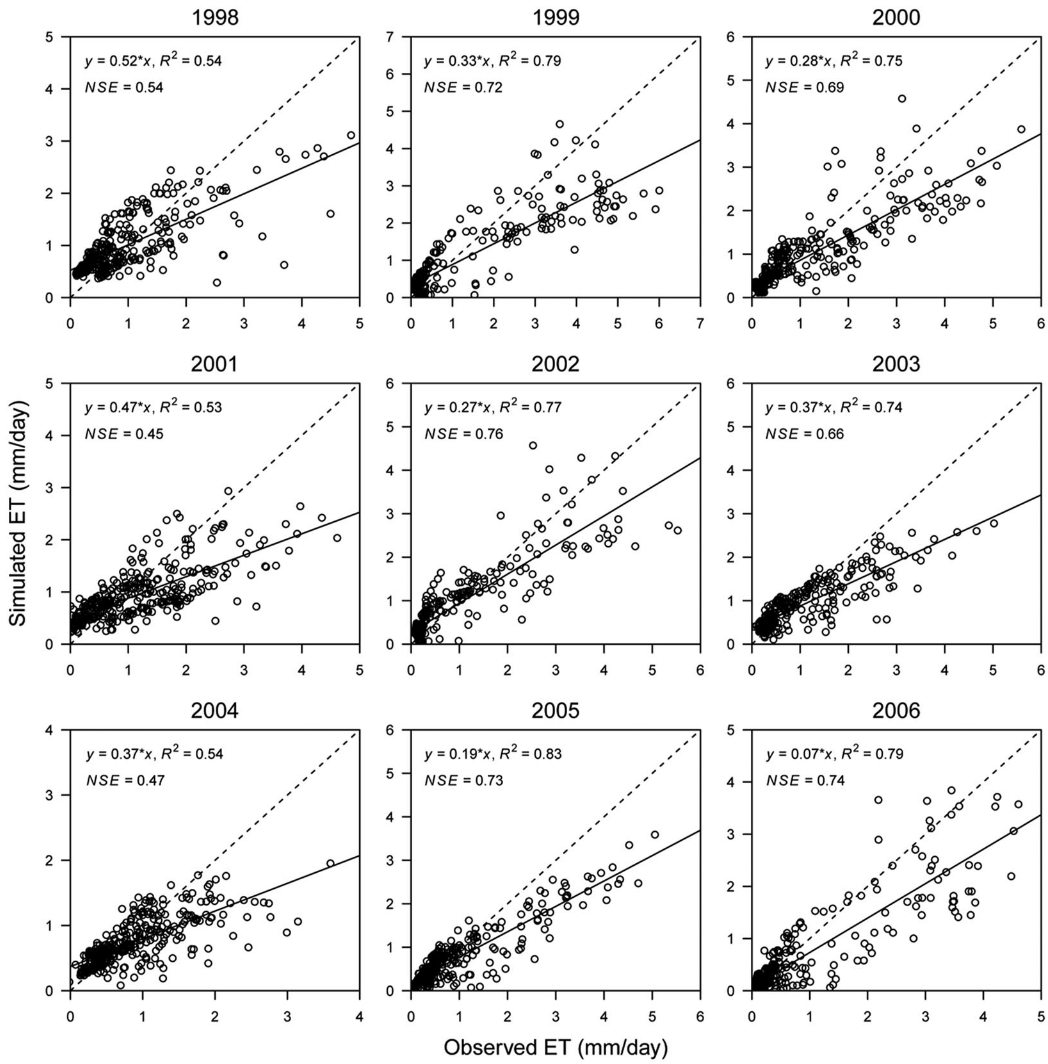

Figure 4. Scattered plots of observed and simulated ET.

As seen in Figure 3(b), the simulated values follow the seasonal dynamic of satellite-derived M_A, which indicates that the VOM model can well capture the temporal variation of the foliage vegetation cover. However, simulated M_A is much lower than satellite-derived M_A in the non-growing season. This indicates that the model underestimates vegetation growth in spring or winter. In addition, the peak of the vegetation cover fraction of the site achieves 1.0 for a longer period than the satellite-derived M_A. The unreasonable description of M_A would lead to a deficiency of ET and *T/ET* ratio simulation.

The parameter of slope between ET and carbon assimulation λ_s (Figure 3(c)) responses dramatically to pulses of rainfall and suction head of the top soil layer (Figure 3(d)). The λ_s peaks in the wet season and declines in the dry season indicating that the plants have a higher water use efficiency in the dry season than that in the wet season. With the same soil moisture, the shrub produces more carbon in the dry season than in the wet season. The optimized parameters $c_{\lambda f,\ s}$ and $c_{\lambda e,\ s}$ are 411.7 and −0.88. Both the two parameters are higher than that of C4 grass in Savannah site reported by Schymanski et al. (2009). This is realistic as plants in semiarid has a higher water use efficiency than that of sub-humid plants.

3. Results and discussion

3.1. ET

For ET partitioning, we first need to validate the model's ability to produce reasonable ET and ET dynamic. ET measurements from Lucky Hills site are used for model validation. Figure 4 shows the scattered plots of simulated and observed daily ET for each year from 1998 to 2006. Most of the years

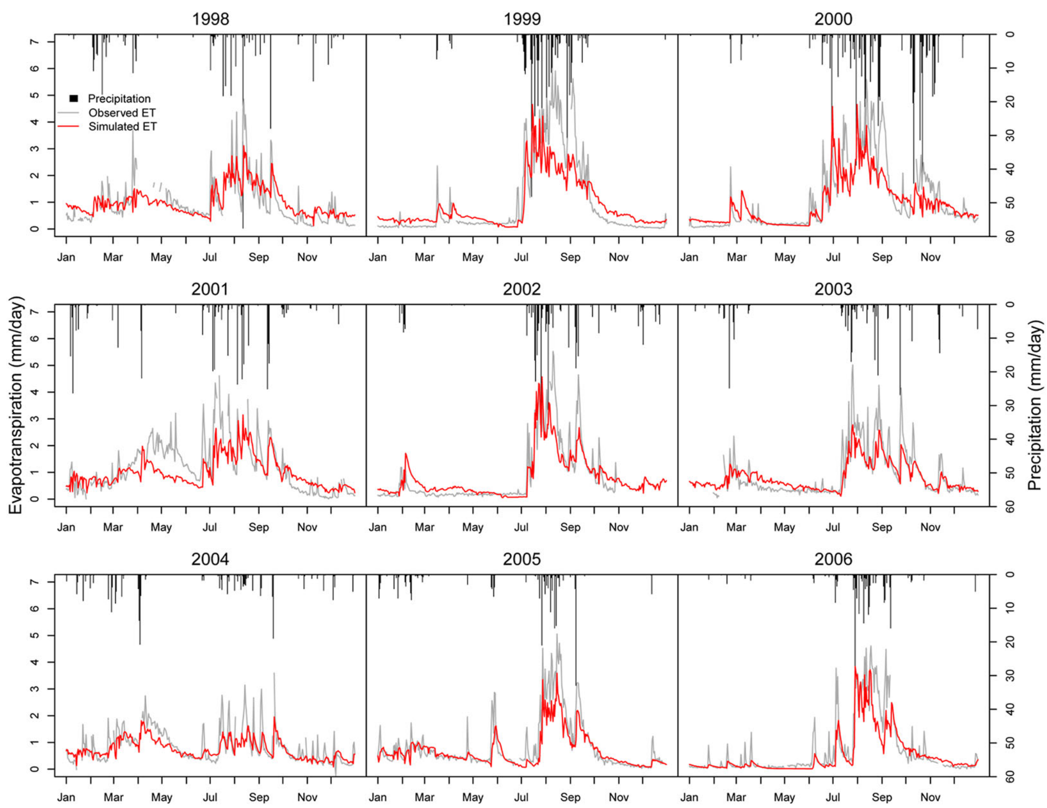

Figure 5. Comparison of observed and simulated daily ET.

are simulated well with the dots distributed along the 1:1 lines. The observed values and simulated values have a relatively good correlation with R square higher than 0.8 for all of the years. The Nash–Sutcliffe coefficient, widely used in hydrology for modeling assessment, is applied to evaluate the difference between simulated and observed values. The Nash–Sutcliffe coefficient of the model fit is higher than 0.7 in 1999, 2002, 2005, and 2006, indicating the results are reliable in these years. The simulated ET in the rest of the years demonstrate acceptable Nash–Sutcliffe coefficient that is higher than 0.5, except for the year of 2001 and 2004.

Figure 5 illustrates the dynamics of the simulated and observed ET for each year. In general, the variation pattern of the simulated ET corresponds with the measured ET. The model is able to capture the ET dynamic reasonably well in response to precipitation events. For example, when rainfall occurs ET occurs, and simulated ET is mainly concentrated in the monsoon when rainfall concentrates. In this way, these results indicate that the model has the capability to capture the daily dynamic ET sufficiently well. However, we also find a tendency of underestimation of ET in some years. As seen in Figure 5, in 2004, simulated ET is much lower than the observed ET, with a Nash–Sutcliffe coefficient of 0.47. This might be due to the unreasonable prediction of vegetation cover as it underestimates vegetation in non-growing season.

3.2. ET Partitioning

The results of daily evaporation and transpiration simulated by the VOM model are shown in Figure 6. Evaporation and transpiration show similar seasonal dynamic pattern during the study period, which mainly occurs in monsoon following the precipitation events. Evaporation responds

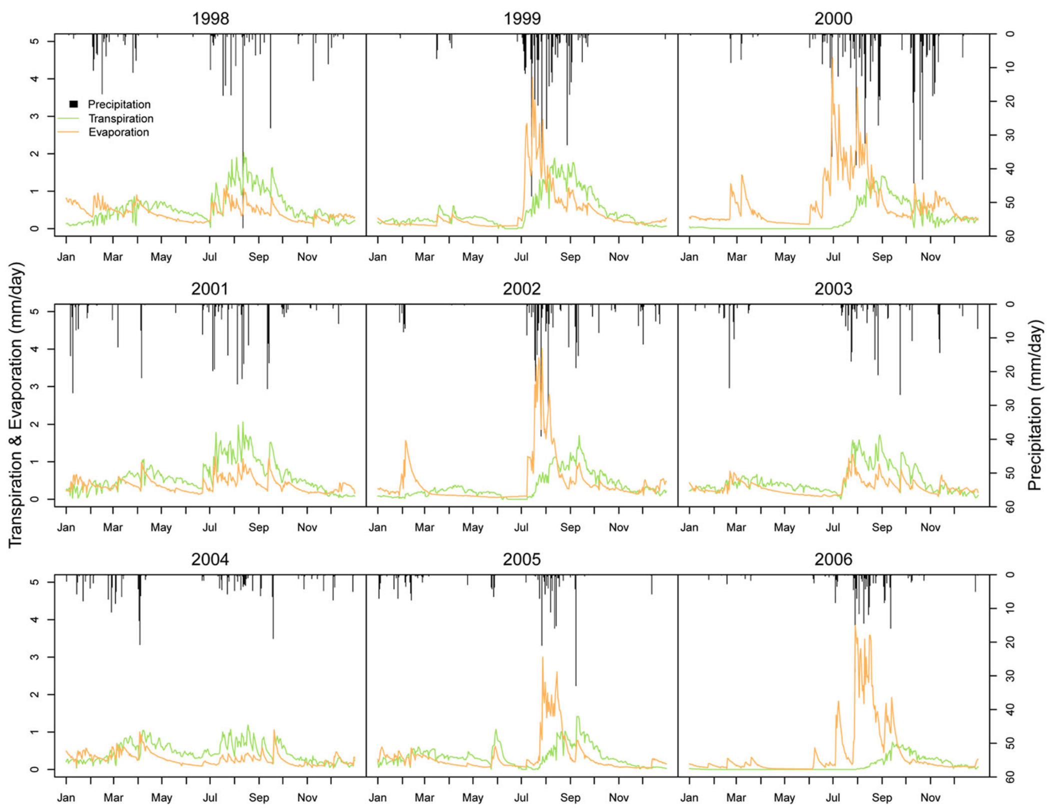

Figure 6. Daily evaporation and transpiration simulated by VOM model.

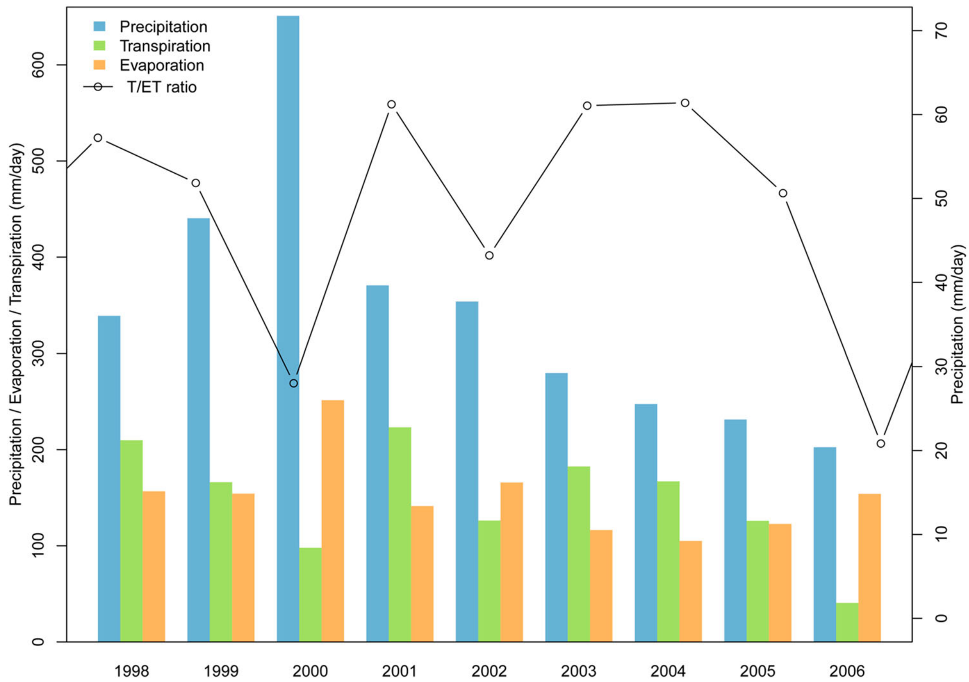

Figure 7. ET partitioning on a yearly scale.

immediately to precipitation events, while transpiration shows a lagged response to those events. In spring and winter, both evaporation and transpiration equal approximately zero for most of the time. When it rains in spring or winter, ET is mainly dominated by evaporation. In the monsoon, when the plants begin to grow after an accumulation of moisture, transpiration increases quickly and dominates ET. Such results are consistent with the results of Scott et al. (2006).

Generally, plant transpiration accounts for 49% of the total ET for the period from 1998 to 2006. This is essentially in agreement with the results of Kemp et al. (1997) that in Chihuahuan Desert communities the *T/ET* ratio ranges from 40% to 60%. Likewise, Scott et al. (2006) partition the ET into evaporation and transpiration for the 2003 growing season in Lucky Hills site using the Bowen ratio and sap-flow method. They found that vegetation transpiration comprises 58% of the total ET, which is consistent with 61% in 2003 estimated by this study. *T/ET* ratio varies dramatically among different years, from 21% to 61% (Figure 7). In 2006, only 21% of yearly ET is plant transpiration, while in 2001, 2003, and 2004, 61% of yearly ET is plant transpiration. Compared to the precipitation of each year, there is no evident relationship with the amount of precipitation. Years with a large amount of precipitation or a small amount of precipitation could have the same *T/ET* ratio. For example, 2001 with yearly precipitation of 370.6 mm has the same *T/ET* ratio with 2004 with a precipitation of 247.39 mm. To further examine the relationship of *T/ET* ratio with the amount of precipitation, we subdivide the data into two groups, one with precipitation higher than average yearly precipitation (1998, 1999, 2000, 2004 and 2006), and the other with precipitation lower than average precipitation (2001, 2002, 2003, and 2005). The average *T/ET* ratio of the group with higher precipitation is 44%, and average *T/ET* ratio of the group with lower precipitation is 54%. Therefore, there is an overall tendency that low yearly precipitation has a higher *T/ET* ratio.

T/ET ratio and its dynamic in the monsoon (from July to September) is showed in Figure 8. Monthly *T/ET* ratio varies from 0 to 74% with a mean value of 48%. Transpiration mainly occurs in August and September, which account for 51% and 63%, respectively. Though precipitation in

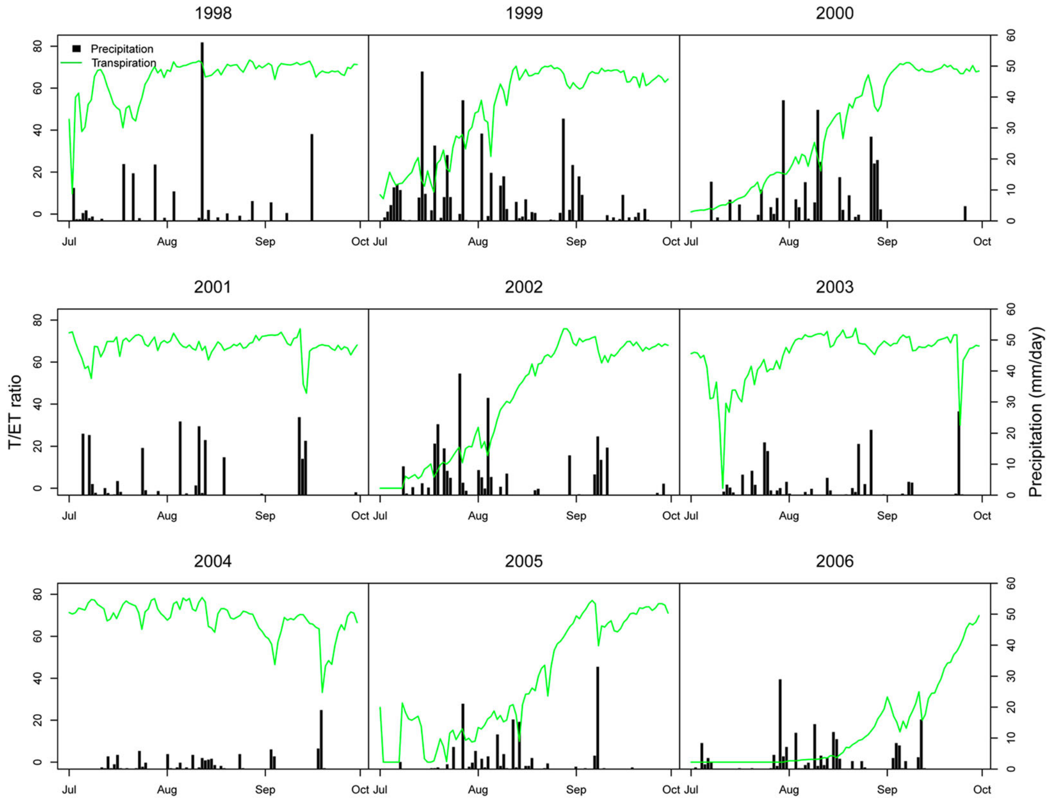

Figure 8. Simulated daily evaporation and transpiration in monsoon.

July is approximately equal to that of August, plant transpiration is much lower in July with a *T/ET* ratio of 35%. This is because the plants need time to develop roots and leaves before it becomes active, and before that precipitation are mainly used for by soil evaporation.

Figure 9 illustrates monthly averaged evaporation and transpiration in monsoon. As seen in Figure 9, *T/ET* ratio dynamic in monsoon demonstrates different patterns. Some of the years (1999, 2000, 2002, 2005, and 2006), show low *T/ET* ratio at the beginning of the monsoon and an increased trend of *T/ET* ratio during the monsoon. The peak of the *T/ET* ratio lags behind the rain events, thus, it does not appear concurrently with the peak of precipitation. For instance, in 1999, plant transpiration only accounts for 24% of monthly ET in July and its peak occurs in August, though the maximum precipitation occurs in July. Four of the nine years (1998, 2001, 2003, and 2004) demonstrate stable and relatively high *T/ET* ratio during the monsoon. *T/ET* ratios of the four years are all higher than 60% during monsoon.

3.3. Impact of precipitation on ET partitioning

In semiarid ecosystems, precipitation is the major driver of plant growth. Seasonal timing, frequency and amount of precipitation have a great influence on the *T/ET* ratio. In this site, the monsoon provides the majority of the precipitation, ranging from 94 mm to 415 mm, as a result, the evaporation and transpiration correspondingly mainly occur in the monsoon. Evaporation responds to the summer precipitation immediately that peaks on the day or the day following the rain pulse, and then declined in the following days immediately. The peak of transpiration lags behind the evaporation, the lag time varies from year to year.

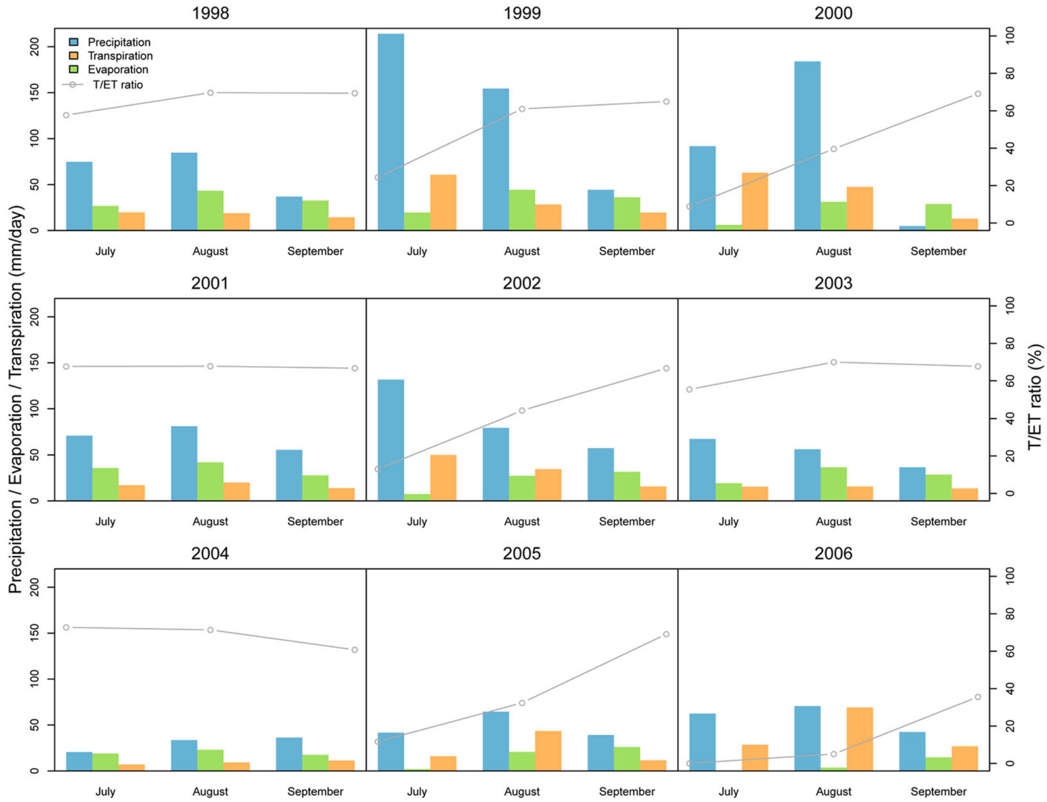

Figure 9. Monthly averaged evaporation and transpiration in monsoon.

As seen in Figures 8 and 9, five years (1999, 2000, 2002, 2005 and 2006) demonstrate a low *T/ET* ratio at the onset of monsoon and a continuous increasing *T/ET* ratio during the monsoon. We can find these years have dry spring with extremely low spring precipitation except for 2005, ranging from 8 mm to 30 mm. With respect to the size of precipitation, we can find that there is no rain event with size >10 mm in these years (Table 5). 0–5 mm size class precipitation is the dominant size class. Even though 2005 has 80 mm spring precipitation, the size of each rain pulse is small, most of which are fell in the 0–5 mm size class. As a result, shrubs in this site remain inactive and there is no evident CO_2 uptake during the spring (Figure 10). Under such circumstances, when summer rains arrived, the shrub has not grown yet; so most rains are consumed by soil evaporation. It takes a long time for plants to recover from growth and respond to the summer precipitation. Therefore, the soil evaporation constitutes the majority of evapotranspiration at the onset of monsoon showing low *T/ET* ratio, and after shrubs have developed leaves and roots, transpiration starts to dominate evapotranspiration showing a high *T/ET* ratio.

In contrast, the four years (1998, 2001, 2003 and 2004) with high *T/ET* during the monsoon all have spring precipitation with size >10 mm (Table 5). 10 mm class size might be the efficient precipitation for shrub growth in this area. As seen in Figure 10, there is evident CO_2 uptake except for 2003. For instance, 2001 demonstrates the highest spring precipitation of the nine years, and after the accumulation of soil moisture, shrubs recover and begin to grow, which lead to obvious carbon sink in April and May. As shrubs have developed a certain number of roots and leaves, when summer rains come, transpiration remains a certain amount. In contrast, soil evaporation peaks on the rainy day or one day following, and then declines quickly.

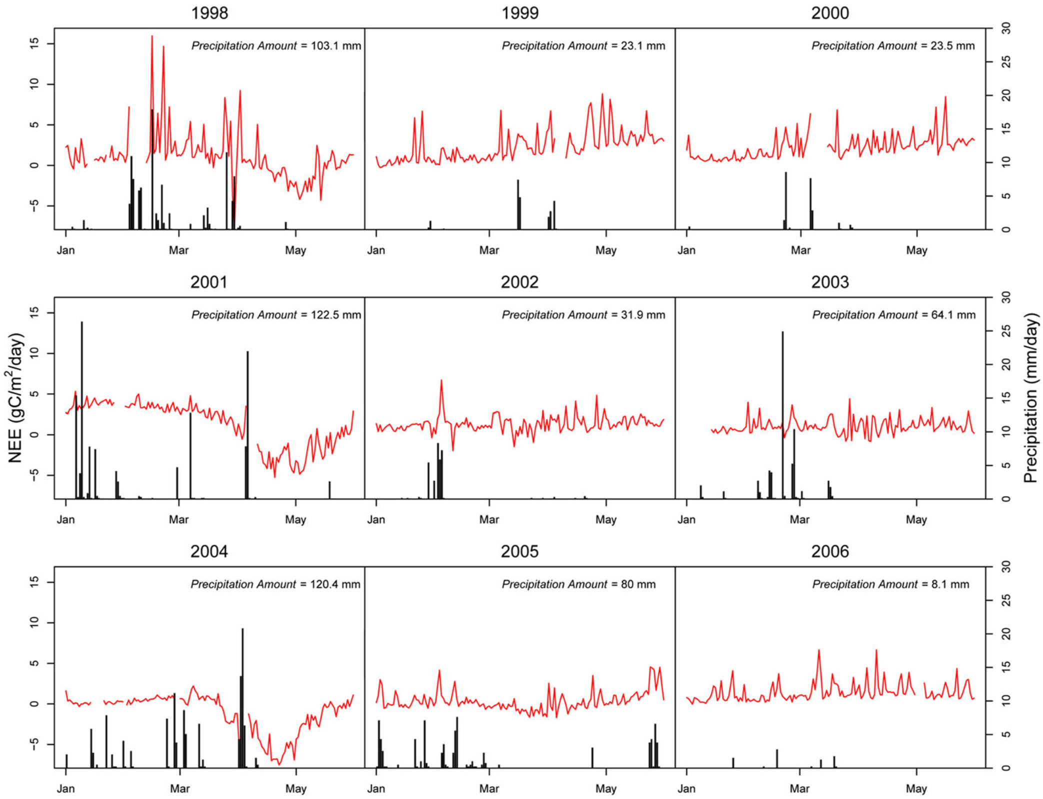

Figure 10. Spring precipitation and CO_2 uptake.

Therefore, the *T/ET* ratio declined on the rainy day and increased quickly as soil evaporation declined quickly. As a result, *T/ET* ratio declines on the rainy day, increased quickly after soil evaporation declined and then keeps high during inter-storm periods. Interestingly, we find 2003 as an exception, which does not have evident CO_2 uptake in the spring, but the shrubs recover quickly after the first rain event. This might because shrubs have developed certain roots and limited leaves in spring; so there is no significant CO_2 uptake in spring but the developed roots make them easily recover in monsoon.

The impact of spring precipitation on summer transpiration is in agreement with Emmerich and Verdugo (2008), which states that the presence or absence of spring CO_2 uptake has an impact on a threshold value of summer precipitation for shrubs' growth. Years with spring CO_2 uptake tend to

Table 5. Days and amount of spring precipitation by size class.

	Size class (mm)			
Year	0–5 Days/amount (mm)	5–10 Days/amount (mm)	>10 Days/amount (mm)	Total days/total amount (mm)
1998	**28/28.4**	**5/34.3**	**3/40.4**	**36/103.1**
1999	8/15.6	1/7.4	0/0	9/23.0
2000	8/7.2	2/16.3	0/0	10/23.5
2001	**23/22.9**	**3/23.1**	**4/76.6**	**30/122.6**
2002	13/5	4/26.9	0/0	17/31.9
2003	**20/23.5**	**1/5.3**	**2/35.3**	**23/64.3**
2004	**19/26.9**	**7/47.8**	**3/45.7**	**29/120.4**
2005	32/46	5/34	0/0	37/80
2006	7/8.1	0/0	0/0	7/8.1

have a low threshold value for shrub growth, while years without spring CO_2 uptake have a high threshold value.

Most of the studies demonstrate that annual precipitation is the dominant factor for vegetation growth in grassland or shrub land ecosystem (Flanagan, Weaver, and Carlson 2002; Khumalo and Holechek 2005). From this study, combined with some of the other research (Xu and Baldocchi 2004; Emmerich and Verdugo 2008), we can see that spring precipitation plays a more significant role in vegetation in the water-limited area. It makes a difference for vegetation carbon uptake whether there is a great amount of precipitation in spring or not. The size and frequency of rainfall event also have influence on vegetation. Apart from these characteristics, some studies find that the first storm has an important influence. This is due to the high summer ET and quickly dried soil in a semiarid ecosystem. For example, after a summer rainfall, soil evaporation is extremely high and soil quickly becomes dry if there is little vegetation. Therefore vegetation grows slowly as soil water is limited. In contrast, if there is spring rainfall, ET in spring is much lower than in summer. Therefore, after a rainfall, soil can remain wet for vegetation to grow and develop root tissues. When summer rainfall comes, vegetation can uptake a certain amount of soil water during the rainfall event, which makes vegetation grow quickly in the summer.

4. Conclusion

In this paper, we conduct a study of ET partitioning in a semiarid shrubland with an optimality-based ecohydrological model. We use 9 years' detailed measurements to drive the model and validate ET results. We then analyze the characteristic of evaporation, transpiration and their response to precipitation on different time scales. We then examine the influence of precipitation characteristic on monsoon *T/ET* ratio, especially the absence or presence of spring precipitation. The results show that the VOM model can reasonably predict ET and ET components in semiarid shrubland. Evaporation and plant transpiration show similar seasonal dynamic pattern during the study period. Evaporation and plant transpiration mainly occur in monsoon following the precipitation events. Evaporation responds immediately to precipitation events, while transpiration shows a lagged response of several days to those events. Overall, the ratio of transpiration to evapotranspiration is 49% for the study period. The *T/ET* ratio varies among years with the peak of 61%. Different years demonstrate different patterns of *T/ET* ratio dynamic in monsoon. Some of the years show a low *T/ET* ratio at the beginning of monsoon and slowly increased *T/ET* ratio. The other years show high level of *T/ET* ratio for the whole monsoon. We find out that spring precipitation, especially the size of the precipitation, has a significant influence on the *T/ET* ratio in monsoon.

This study has demonstrated the advantages of using the ecohydrological model for ET partitioning. In the future, the model can be applied to explore the optimum water use, transpiration, and evaporation under different climate conditions to deepen our understanding of global climate change on evaporation and transpiration.

Disclosure statement

No potential conflict of interest was reported by the authors.

Funding

This work is supported by the National Key Research and Development Program of China [grant number 2017YFC050540503]; National Natural Science Foundation of China [grant numbers 41301028, 41571413, 41701520 and 41471368]. Lajiao Chen (201704910065) would like to acknowledge the fellowship from the China Scholarship Council (CSC).

References

Biederman, J. A., R. L. Scott, T. W. Bell, D. R. Bowling, S. Dore, J. Garatuza-Payan, and T. E. Kolb, et al. 2017. “CO_2 Exchange and Evapotranspiration Across Dryland Ecosystems of Southwestern North America.” *Global Change Biology* 23 (10): 4204–4221.

Cao, L., G. Bala, K. Caldeira, R. Nemani, and G. Ban-Weiss. 2010. “Importance of Carbon Dioxide Physiological Forcing to Future Climate Change.” *Proceedings of the National Academy of Sciences* 107 (21): 9513–9518.

Cavanaugh, M. L., S. A. Kurc, and R. L. Scott. 2011. “Evapotranspiration Partitioning in Semiarid Shrubland Ecosystems: A two-Site Evaluation of Soil Moisture Control on Transpiration.” *Ecohydrology* 4: 671–681. doi:10.1002/eco.157.

Caylor, K. K., T. M. Scanlon, and I. Rodriguez-Iturbe. 2009. “Ecohydrological Optimization of Pattern and Processes in Water-Limited Ecosystems: A Trade-off-Based Hypothesis.” *Water Resources Research* 45 (W08407), doi:10.1029/2008WR007230.

Cowan, I. R., and G. D. Farquhar. 1977. “Stomatal Function in Relation to Leaf Metabolism and Environment.” In *Integration of Activity in the Higher Plant*, edited by D. H. Jennings, 471–505. Cambridge: Cambridge University Press.

Dirmeyer, P. A., X. Gao, M. Zhao, Z. Guo, T. Oki, and N. Hanasaki. 2006. “GSWP2: Multimodel Analysis and Implications for our Perception of the Land Surface.” *Bulletin of the American Meteorological Society* 87: 1381–1398.

Domec, J. C., G. Sun, A. Noormets, M. J. Gavazzi, E. A. Treasure, E. Cohen, J. J. Swenson, S. G. McNulty, and J. S. King. 2012. “A Comparison of Three Methods to Estimate Evapotranspiration in two Contrasting Loblolly Pine Plantations: Age-Related Changes in Water use and Drought Sensitivity of Evapotranspiration Components.” *Forest Science* 58: 497–512.

Duan, Q. Y., V. K. Gupta, and S. Sorooshian. 1993. “Shuffled Complex Evolution Approach for Effective and Efficient Global Minimization.” *Journal of Optimization Theory and Applications* 76 (3): 501–521.

Duan, Q. Y., S. Sorooshian, and V. K. Gupta. 1994. “Optimal use of the SCE-UA Global Optimization Method for Calibrating Watershed Models.” *Journal of Hydrology* 158 (3-4): 265–284.

Eagleson, P. S. 2002. *Ecohydrology: Darwinian Expression of Vegetation Form and Function*. Cambridge: Cambridge University Press.

Emmerich, W. E., and C. L. Verdugo. 2008. “Long-term Carbon Dioxide and Water Flux Database, Walnut Gulch Experimental Watershed, Arizona, United States.” *Water Resources Research* 44: W05S09. doi:10.1029/2006WR005693.

Evett, S. R., and R. J. Lascano. 1993. “ENWATBAL.BAS: a Mechanistic Evapotranspiration Model Written in Compiled BASIC.” *Agronomy Journal* 85: 763–772.

Evett, S. R., A. W. Warrick, and A. D. Matthias. 1995. “Wall Material and Capping Effects on Microlysimeter Temperatures and Evaporation.” *Soil Science Society of America Journal* 59: 329–336.

Falge, E., D. D. Baldocchi, R. Olson, P. Anthoni, M. Aubinet, C. Bernhofer, G. Burba, et al. 2001. “Gap Filling Strategies for Defensible Annual Sums of Net Ecosystem Exchange.” *Agricultural and Forest Meteorology* 107: 43–69.

Flanagan, L. B., L. A. Weaver, and P. J. Carlson. 2002. “Seasonal and Interannual Variation in Carbon Dioxide Exchange and Carbon Balance in a Northern Temperate Grassland.” *Global Change Biology* 8: 599–615.

Goodrich, D. C., T. O. Keefer, C. L. Unkrich, M. H. Nichols, H. B. Osborn, J. J. Stone, and J. R. Smith. 2008. “Long-term Precipitation Database, Walnut Gulch Experimental Watershed, Arizona, United States.” *Water Resources Research* 44: W05S04. doi:10.1029/2006WR005782.

Keefer, T. O., M. S. Moran, and G. B. Paige. 2008. “Long-term Meteorological and Soil Hydrology Database, Walnut Gulch Experimental Watershed, Arizona, United States.” *Water Resources Research* 44: W05S07. doi:10.1029/2006WR005702.

Kemp, P. R., J. F. Reynolds, Y. Pachepsky, and J. L. Chen. 1997. “A Comparative Modeling Study of Soil Water Dynamics in a Desert Ecosystem.” *Water Resources Research* 33 (1): 73–90.

Kerkhoff, A. J., S. N. Martens, and B. T. Milne. 2004. “An Ecological Evaluation of Eagleson’s Optimality Hypotheses.” *Functional Ecology* 18: 404–413.

Khumalo, G., and J. Holechek. 2005. “Relationship Between Chihuahuan Desert Perennial Grass Production and Precipitation.” *Rangeland Ecological Management* 58: 239–246.

Kool, D., N. Agam, N. Lazarovitch, J. L. Heitman, T. J. Sauer, and A. Ben-Gal. 2014. “A Review of Approaches for Evapotranspiration Partitioning.” *Agricultural and Forest Meteorology* 184: 56–70.

Lawrence, D. M., P. E. Thornton, K. W. Oleson, and G. B. Bonan. 2007. “The Partitioning of Evapotranspiration into Transpiration, Soil Evaporation, and Canopy Evaporation in a GCM: Impacts on Land-Atmosphere Interaction.” *Journal of Hydrometeorology* 8 (4): 862–880. doi:10.1175/JHM596.1.

Lei, H., D. Yang, S. J. Schymanski, and M. Sivapalan. 2009. “Modeling the Crop Transpiration Using an Optimality-Based Approach.” *Science in China Series E: Technological Sciences* 51 (S2): 60–75.

Newman, B. D., B. P. Wilcox, S. R. Archer, D. D. Breshears, C. N. Dahm, C. J. Duffy, N. G. McDowell, F. M. Phillips, B. R. Scanlon, and E. R. Vivoni. 2006. “Ecohydrology of Water-Limited Environments: A Scientific Vision.” *Water Resources Research* 42: W06302.

Oki, T., and S. Kanae. 2006. “Global Hydrological Cycles and World Water Resources.” *Science* 313 (5790): 1068–1072.
Pauwels, V. R. N., N. E. C. Verhoest, G. J. M. De Lannoy, V. Guissard, C. Lucau, and P. Defourny. 2007. “Optimization of a Coupled Hydrology-Crop Growth Model Through the Assimilation of Observed Soil Moisture and Leaf Area Index Values Using an Ensemble Kalman Filter.” *Water Resources Research* 43. doi:10.1029/2006WR004942.
Ponce-Campos, G. E., M. S. Moran, A. Huete, Y. Zhang, C. Bresloff, T. E. Huxman, D., Eamus, D. D., et al. 2013. “Ecosystem Resilience Despite Large-Scale Altered Hydroclimatic Conditions.” *Nature* 494 (7437): 349–352.
Raz-Yaseef, N., D. Yakir, G. Schiller, and S. Cohen. 2012. “Dynamics of Evapotranspiration Partitioning in a Semi-Arid Forest as Affected by Temporal Rainfall Patterns.” *Agricultural and Forest Meteorology* 157: 77–85.
Rodriguez-Iturbe, I., and A. Porporato. 2004. *Ecohydrology of Water-Controlled Ecosystems*. Cambridge: Cambridge University Press.
Schymanski, S. J., M. L. Roderick, M. Sivapalan, L. B. Hutley, and J. Beringer. 2007. “A Test of the Optimality Approach to Modelling Canopy Properties and CO_2 Uptake by Natural Vegetation.” *Plant, Cell & Environment* 30 (12): 1586–1598.
Schymanski, S. J., M. Sivapalan, M. L. Roderick, L. Hutley, and J. B. Beringer. 2009. “An Optimality-Based Model of the Dynamic Feedbacks Between Natural Vegetation and the Water Balance.” *Water Resources Research* 45: W01412. doi:10.1029/2008 WR006841.
Scott, R. L., and J. A. Biederman. 2017. “Partitioning Evapotranspiration Using Long-Term Carbon Dioxide and Water Vapor Fluxes.” *Geophysical Research Letters* 44: 6833–6840. doi:10.1002/2017GL074324.
Scott, R. L., T. E. Huxman, W. L. Cable, and W. E. Emmerich. 2006. “Partitioning of Evapotranspiration and its Relation to Carbon Dioxide Exchange in a Chihuahuan Desert Shrubland.” *Hydrological Processes* 20: 3227–3243.
Scott, R. L., J. S. Shuttleworth, T. O. Keefer, and A. W. Warrick. 2000. “Modeling Multiyeal Observations of Soil Moisture Recharge in the Semiarid American Southwest.” *Water Resources Research* 36 (8): 2233–2247.
Shuttleworth, W. J., and J. S. Wallace. 1985. “Evaporation From Sparse Crops – an Energy Combination Theory.” *Quarterly Journal of the Royal Meteorological Society* 111: 839–855.
Sivapalan, M. 2009. “The Secret to ‘Doing Better Hydrological Science’: Change the Question!.” *Hydrological Processes* 23 (9): 1391–1396.
Thompson, A. L., D. L. Martin, J. M. Norman, J. A. Tolk, J. R. Gilley, and A. D. Schneider. 1997. “Testing of a Water Loss Distribution Model for Moving Sprinkler Systems.” *Transactions of the ASAE* 40: 81–88.
Todd, R. W., S. R. Evett, T. A. Howell, and N. L. Klocke. 2000. “Soil Temperature and Water Evaporation of Small Steel and Plastic Lysimeters Replaced Daily.” *Soil Science* 165: 1–2.
Trenberth, K. E., J. T. Fasullo, and J. Kiehl. 2009. “Earth’s Global Energy Budget.” *Bulletin of the American Meteorological Society* 90: 311–324.
Van der Tol, C., A. J. Dolman, M. J. Waterloo, and C. A. Meesters. 2008. “Optimum Vegetation Characteristics, Assimilation, and Transpiration During a dry Season: 2. Model Evaluation.” *Water Resources Research* 44: W03421. doi:10.1029/2007 WR006243.
Wang, J., R. L. Bras, M. Lerdau, and G. D. Salvucci. 2007. “A Maximum Hypothesis of Transpiration.” *Journal of Geophysical Research* 112. doi:10.1029/2006JG000255.
Wang, L., K. K. Caylor, J. C. Villegas, G. A. Barron-Gafford, D. D. Breshears, and T. E. Huxman. 2010. “Partitioning Evapotranspiration Across Gradients of Woody Plant Cover: Assessment of a Stable Isotope Technique.” *Geophysical Research Letters* 37: L09401. doi:10.1029/2010GL043228.
Wang, K., and R. E. Dickinson. 2012. “A Review of Global Terrestrial Evapotranspiration: Observation, Modeling, Climatology, and Climatic Variability.” *Reviews of Geophysics* 50 (2). doi:10.1029/2011RG000373.
Xu, L., and D. D. Baldocchi. 2004. “Seasonal Variation in Carbon Dioxide Exchange Over a Mediterranean Annual Grassland in California.” *Agricultural and Forest Meteorology* 123: 79–96.
Zhou, S., B. F. Yu, Y. Zhang, Y. F. Huang, and G. Q. Wang. 2016. “Partitioning Evapotranspiration Based on the Concept of Underlying Water use Efficiency.” *Water Resources Research* 52: 1160–1175. doi:10.1002/2015WR017766
Zhou, S., B. Yu, Y. Zhang, Y. Huang, and G. Wang. 2018. Water use Efficiency and Evapotranspiration Partitioning at Three Typical Ecosystems in the Heihe River Basin.” *Agricultural and Forest Meteorology* 253-254: 261–273. doi:10.1016/j.agrformet.2018.02.002.